ARCNL

Internship report

Substrate Wear Accompanying Vibration Induced Friction Reduction by Quartz Crystal Microbalances

Minimizing the friction between theory and experiment

Author:
Vincent Benning BSc

Supervisors:
Dr. Bart Weber
Dr. Felix Cassin

August 28, 2021

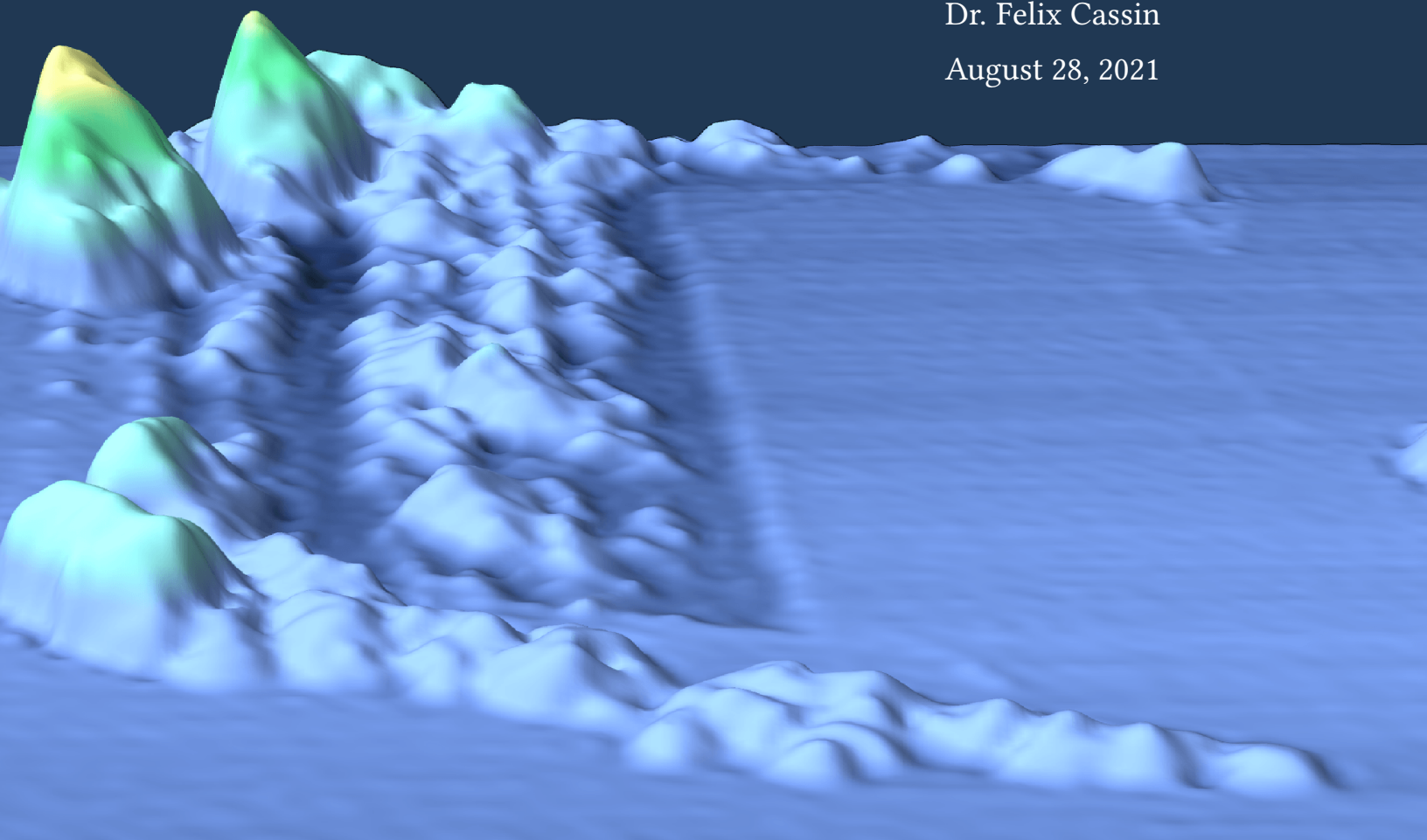

Abstract

With the implementation of quartz crystal microbalance (QCM) in atomic force microscopy (AFM) setups it became possible to study friction and wear on microscopic scales at high sliding speeds. Development of the technique revealed that the QCM also alters the observed friction, with the capability to achieve superlubricity. These QCM-induced friction reduction phenomena have been investigated extensively. However, these studies focus little on the wear accompanying QCM sliding experiments. Hence, in this report we provide a preliminary study on the relation between wear and friction for QCM coupled sliding interfaces.

For this work we show the response of atomically flat MoS_2, Si and Au/Cr to a single abrasive diamond asperity sliding over the substrate surfaces, in the presence and absence of QCM-induced oscillations of around 5 MHz. These substrates often find application in tribolgy research and were therefore chosen as case studies. To simulate the sliding asperity, a diamond tipped AFM probe in contact mode was used. During the wear test a 60 μN normal load was applied with a 1Hz line rate in a $2\mu m \times 2\mu m$ area. The displaced material and friction profile of the substrate were mapped using AFM in tapping and contact mode, respectively.

We demonstrate that the wear on all samples is drastically increased when sliding is performed in tandem with QCM-induced vibrations. Integration of the debris volume showed that surface wear increases from a factor 4 to 50 when the QCM is employed during wearing. In line with other research, the friction profiles of the Si and Au substrate were found to drop by a factor of 4. It is noteworthy that a similar effect was not seen for MoS_2. This was attributed to the relative angle between the QCM oscillation and the fast scanning direction of the cantilever.

Contents

1 Introduction

Frictional forces are apparent in everyday life. The force constantly acts as a sink for energy and drives the degradation of moving mechanical components.[1] Hence, advancements in tribology –the study of interacting surfaces in relative motion– may lead to the partial reduction or elimination of unwanted friction phenomena, as well as the associated wear. The importance of such developments can not be understated, whereas this will inevitably have large consequences for the long-term reliability of machines and analogous to the economics of involved industries.[2,3] Although, superficially friction seems to be a straight forward phenomenon, devising a rigorous theoretical framework proves difficult. This stems from the stark difference in quantitative and qualitative behaviour between the macro- and microscopic domain. Where the microscopic scale forces arise from interactions between opposed atomically flat planes, the macroscopic interfaces are comprised of a large set of discrete areas ranging from micro- to nanometers i.e. asperities. Further complexity arises from them all having distinct mechanical responses. Thus, understanding macroscopic friction is not a straightforward extension of the microscopic material characteristics.[4,5]

Recently, research efforts to establish the link between these scales has been placed in a new light, via the introduction of quartz crystal microbalances (QCM) to experimental setups.[5,6] At the heart of the QCM is a crystalline quartz disk with metal electrodes on both faces. When the piezoelectric disk is driven by an AC voltage, it starts to oscillate at its natural frequency producing MHz vibrations.[7] As a result macroscopic scale sliding speeds in the order of 0.1-1 m/s can be attained for microscopic scale contact areas.

A remarkable observation from multiple independent research groups is the friction reduction and even the onset of superlubricity –the near vanishing of sliding friction between two surfaces– for systems coupled with the active vibration of a QCM module. This seems to imply that the friction forces can be manipulated at will, enabling one to tune the friction to accommodate specific scenarios e.g. removing friction when sliding objects past each other. Nonetheless, the origin of this apparent friction decrease is still speculative and poorly understood.[8–10] Recent research by Bhattacharjee, et al found that for Au and MoS_2 superlubricity is achieved for a wide range of experimental variables i.e. probes of 50 to 1500μm and high loads ranging from 20μN to 5mN, but could not reproduce the same result with sharp AFM probes. They hypothesized that this was due to associated probe spring forces being to low compared to the interfacial friction.[9] Wada et al. on the other hand found that super lubrication for MoS_2 is possible with an AFM setup. However, these results were only obtained if the surface was patterned, such that it consisted of free standing islands of 0.2μm in size. This has lead them to state that superlubrication is only possible if the phonons created by stick-slip events are confined within these islands.[11]

The aim of all these works seems predominantly focused on understanding the origin of the QCM-induced superlubricity, however little attention is given to the wearing of probe and substrate employed in their experiments. It is even implied in the works of Bhattacharjee et al. that a decrease in friction automatically leads to decreased wear.[9] Moreover, investigations till now have mainly used tribometers for sample manipulation and friction measurements. However, the amplitude of QCM crystals oscillations have a length scale in the order of nanometers, making AFM with its high spatial resolution a better suited approach to study the phenomenon.[5,6,9]

Therefore, the objective of this report is to resolve the relationship between interfacial wear and friction under QCM vibration. To this end we have performed a study of the substrate wear caused by wearing chromium/gold, MoS_2 and amorphous silicon with a diamond tip AFM probe, in the absence and presence of QCM-induced vibrations. To relate the amount of substrate wear to the friction measured during wearing, we will compare the volume of displaced surface material to the integrated force loop area i.e. friction, measured during the experiment. [1]

Our findings show increased surface wear for experiments with active QCM-induced vibrations, even though a substantial drop in friction is observed for Si and Au/Cr. The origin for this increased wear is attributed to the increased path length caused by crystal oscillations. The friction behaviour can not straightforwardly be explained. It is believed to arise from the interplay between sample location and a friction reduction pathway triggered by the vibrations. The proposed hypothesis will be discussed in detail in Section 3. The results from present report pave the way for a better understanding between QCM vibrations and wear. These result could aid in the development of new cutting technologies, where highly localized wear along a predetermined path is beneficial.

2 Methods

2.1 Materials

The Si and MoS_2substrate samples were prepared from a CONTV-A AFM probe and single crystal MoS_2, purchased from Bruker and Merck, respectively.[2] After processing, these were attached to QCM crystal sensors acquired from INFICON. The crystals were AT-cut, resulting in a pure shear mode vibration with a resonance frequency of 5 MHz. Both faces of the crystals were of plano geometry and were coated with a gold electrode layer. Additionally, a chromium adhesion layer was present on the sensing facet i.e. the facet on which the various substrate samples were adhered. The average surface roughness of the adhesion layer amounted to 5 nm.

For the preparation of the Si sample, the cantilever was separated from the support chip. The choice for a cantilever tip as Si substrate instead of a Si wafer piece was made, because adhesion of the substrate on the QCM crystal proved difficult. It was found that the oscillatory motion of the crystal was hampered when the sample mass was too high and when the adhesive was to stiff .i.e if an epoxy based adhesive was used. Subsequently, a solution of acetone and scotch tape adhesive was dropped on the center of the sensing electrode. The adhesive solution was placed in a clean room for 15 minutes to partially evaporate off and to avoid contamination by airborne dust. The drying step was proceeded by placing the cantilever on the adhesive and pressing it down with a cotton swap. Following the attachment, excessive glue residues was removed, as this impeded the resonance oscillation of the QCM crystal. Figure 1a shows the final Si sample.

Preparation for the MoS_2sample followed a similar protocol for appliance of adhesive on the

[1] we refer to the integrated area between the trace and retrace of the lateral signal from a given data set as the friction. Note however that this value is only proportional to the friction, see Appendix A.2 for the derivation of the relation.

[2] The full overview of the materials can be found in Appendix B

a b

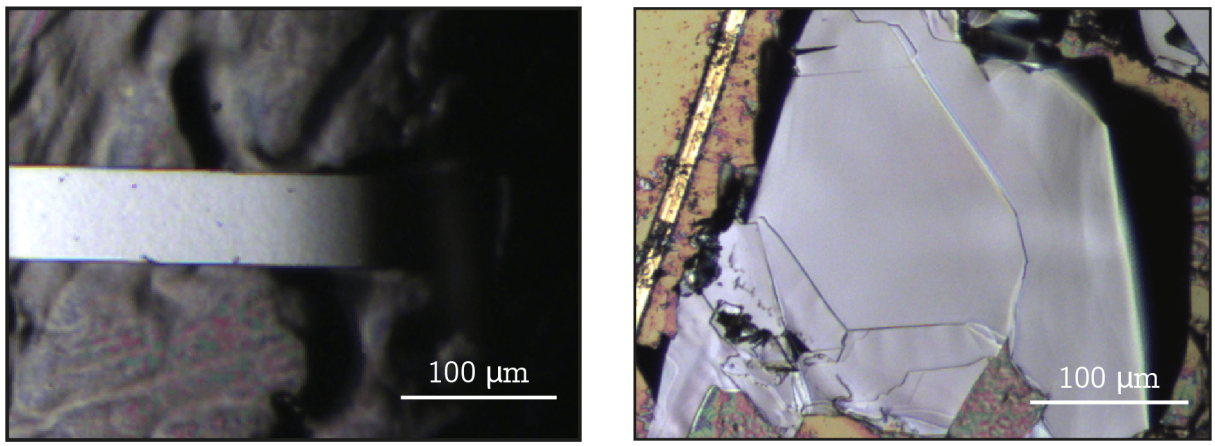

Figure 1. Si and MoS_2sample - Optical microscope image of the **(a)** Si and **(b)** MoS_2substrate adhered to the QCM electrode. The multi-colored residue among the sample borders is excess adhesive.

QCM crystal. A sufficiently light flake of single crystalline MoS_2(approximately $230 \times 265\ \mu m$) was acquired via exfoliation of the single crystal MoS_2sample. Next the exfoliate was pressed on the adhesive for 5 minutes and removed, leaving behind a small multilayered flake of MoS_2. Similarly to the Si sample, excess glue residue was removed until the resonance frequency of the crystal was restored. Analysis with an optical microscope and AFM revealed that the sample consisted of layered planes, which were atomically flat, as shown in Figure 1b.

Preparation of the Cr/Au substrate was simply realized by rinsing the QCM sensing electrode with acetone. The positioning of the Si and MoS_2substrate on the QCM electrode as well as the measurement location of the the Au/Cr substrate, is visualized in Figure 2a

To invoke surface wear, a silicon cantilever with a conically shaped diamond-coated probing tip from Adma Inovations (article code NC-LC) was utilized. The base dimensions were 125 ± 10, 40 ± 5 and $4.0 \pm 0.5\ \mu m$ for the length width and height, respectively with a spring constant of 125 ± 75 N/m. The tip radius amounted to 20 ± 10 nm and featured a full tip angle of $90 \pm 20°$. To ensure sufficient surface wear $60\ \mu N$ of force was applied on the substrate during measurement. The wear series were measured with the same tip on the span of a single day, in the order: Si, MoS_2, Au/Cr. This was to prevent variations in relative humidity and tip mounting between experiments, at the expense of a possible contamination of the substrates with debris from previous runs. Preceding the experiment the probe was calibrated using thermal tuning and subsequent fitting of the generated data using the Sader method.[12] The fitting parameters for the deflection sensitivity and spring constant were in turn used to calculate the voltage set-point, corresponding to $60\ \mu N$ of force.

Analysis of the worn surfaces was performed using AFM in tapping mode. A RTESPA-300 AFM probe from Bruker instruments was utilized for imaging. A similar procedure for calibration and measurement was used as for the surface wearing.

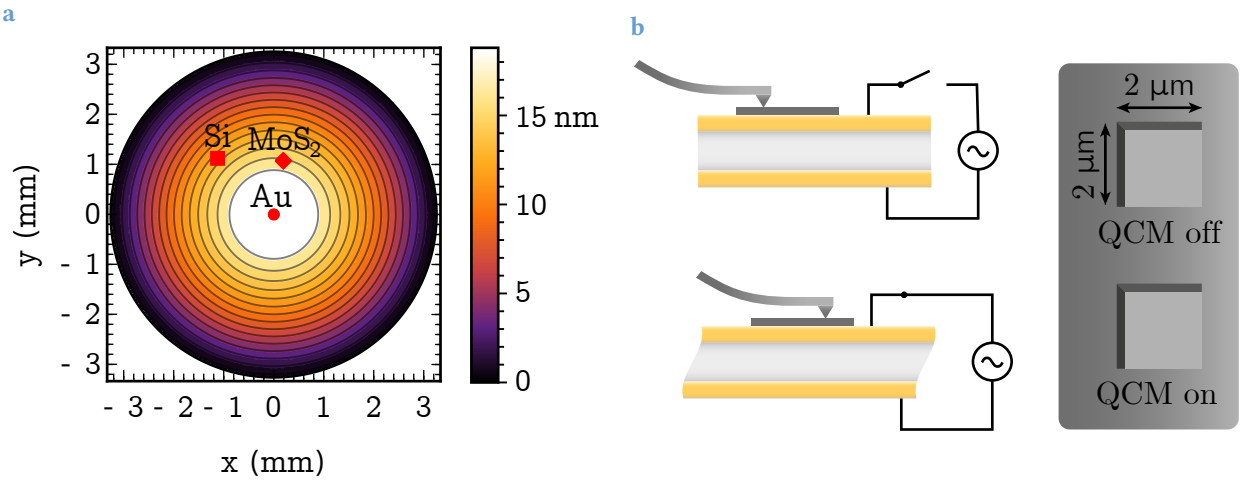

Figure 2. QCM setup - (a) Estimated *QCM amplitude distribution* of shear waves in the absence of any deposited material, modeled using a Bessel function. The amplitude maximum coincides with the center of the QCM front electrode. The spatial extend of the Bessel function is equal in size to the smaller back electrode. The red markings in the plot show the approximate radial position of the analyzed substrate on the QCM crystal. The relative angle varied between experiments **(b)** Experimental setup for wearing the surface. The substrate layer on top of the QCM is worn in a 2 by 2 micron square, while the QCM is on and off.

2.2 Instruments

The lateral forces during probe-substrate sliding and surface topography were measured using a Dimension Icon AFM from Bruker, within a vibration reducing chamber. The AFM mechanics were such that the tip moved while the sample remained stationary. This proved necessary, while AFM with dynamic samples and stationary tips are limited by the sample mass. Therefore, they are not able to accommodate a QCM module. The QCM crystals were driven by Maxtek RQCM system from INFICON, which performed as a phase lock oscillator and frequency measuring module. To accommodate for the size restrains of the AFM apparatus a custom printed crystal holder was constructed. To ensure proper function of the custom holder electronic components of the CHK-100 holder – complementary to the RQCM Maxtek systems – were salvaged and reused. To quantify the oscillatory behaviour of the QCM crystal, the derivation of Martin et al. was used.[13] In there studies they solved the equation of motion for a spherical Plano-Plano quartz disk under the assumption of insignificant energy dissipation and no displacement at the spherical disk boundary. The resulting displacement profile is given by:

$$u(r,t) = u_{max} J_0 \left(2.41 \frac{r}{R}\right) sin(\omega t) \tag{2.1}$$

Where r is the radial position on the crystal, t is the time, u_{max} is the maximum displacement of the crystal, J_0 is the 0 th Bessel function, R is the radius of active oscillation, which corresponds to the radius of the back electrode and ω is the oscillation frequency of the crystal. As an estimate

for the maximum displacement of the QCM we use the derivation of Johannsmann based the transmission line model.[14] This gives the following equation

$$u_{max} = \frac{4}{\pi^2 n^2} d_{AT} Q V \tag{2.2}$$

Where n is the overtone order, d_{AT} is the piezoelectric constant of an AT-cut quartz crystal, Q the quality factor of the QCM crystal and V the amplitude of the driving voltage. Substitution of Equation 2.2 in Equation 2.1 we obtain the displacement profile of the QCM crystal, as visulized in Figure 2a. This theoretical prediction for the maximum amplitude is in line with the experimentally derived formula from Borovsky et al..[7]

2.3 Experimental Design

To test the friction and wear effects caused by the QCM vibrations, the tip was brought in sliding contact with the samples 2 times, once with the QCM on, followed by the control with the QCM off, as is shown in Figure 2b. The designated sample areas were worn by the tip, such that a square pattern with sides of 2 microns were created. The squares consisted of 256 lines in the fast scanning direction. After each wear cycle i.e. a single square pattern, the tip was lifted of the substrate and moved 5 microns in the positive x direction, with reference to the axes of Figure 2a. This resulted in nominally the same vibration amplitude for the new wear site, with at most an amplitude shift of Δu = 0.07 nm. Hence, we can neglect any variation in wear introduced by these different sample locations. The scan rate was 1 Hz, corresponding to a relative sliding speed of 4 $\mu m/s$.

To prevent any further wearing of the sample after the sliding experiments, a compliant cantilever in tapping mode was used for imaging. To obtain high resolution topographic data of the worn surfaces the scan rate was lowered to 0.5 Hz.

3 Results & Discussion

3.1 Friction Profile

The integrated lateral signal for the wear experiments is shown in Figure 3. When the QCM is engaged for the Au/Cr and Si sample the frictions are nominally 31 and 62 percent of the value captured in the absence of vibrations, which is in line with the values reported by previous research of Bhattacharjee et al.[9] Note that the wear increase for Au/Cr from line 20 to 80 is caused by an large surface irregularity in the positive z-direction.

When looking at the MoS_2 sample (Figure 3c) the reverse effect can be observed, where friction is increased by 20 percent with regards to the QCM off experiment. To the authors knowledge this kind of increase in friction invoked by QCM vibrations is not reported before. To exclude unstable surface contact as the cause for the lowered friction, the experiment was repeated for a run where halfway the QCM was turned off. The resulting data is shown in Figure 3d. The large spike in friction is an artifact, created by the damping of the QCM crystal after turning off the alternating voltage. Similarly, we see a friction increase when the QCM is engaged. Preliminary

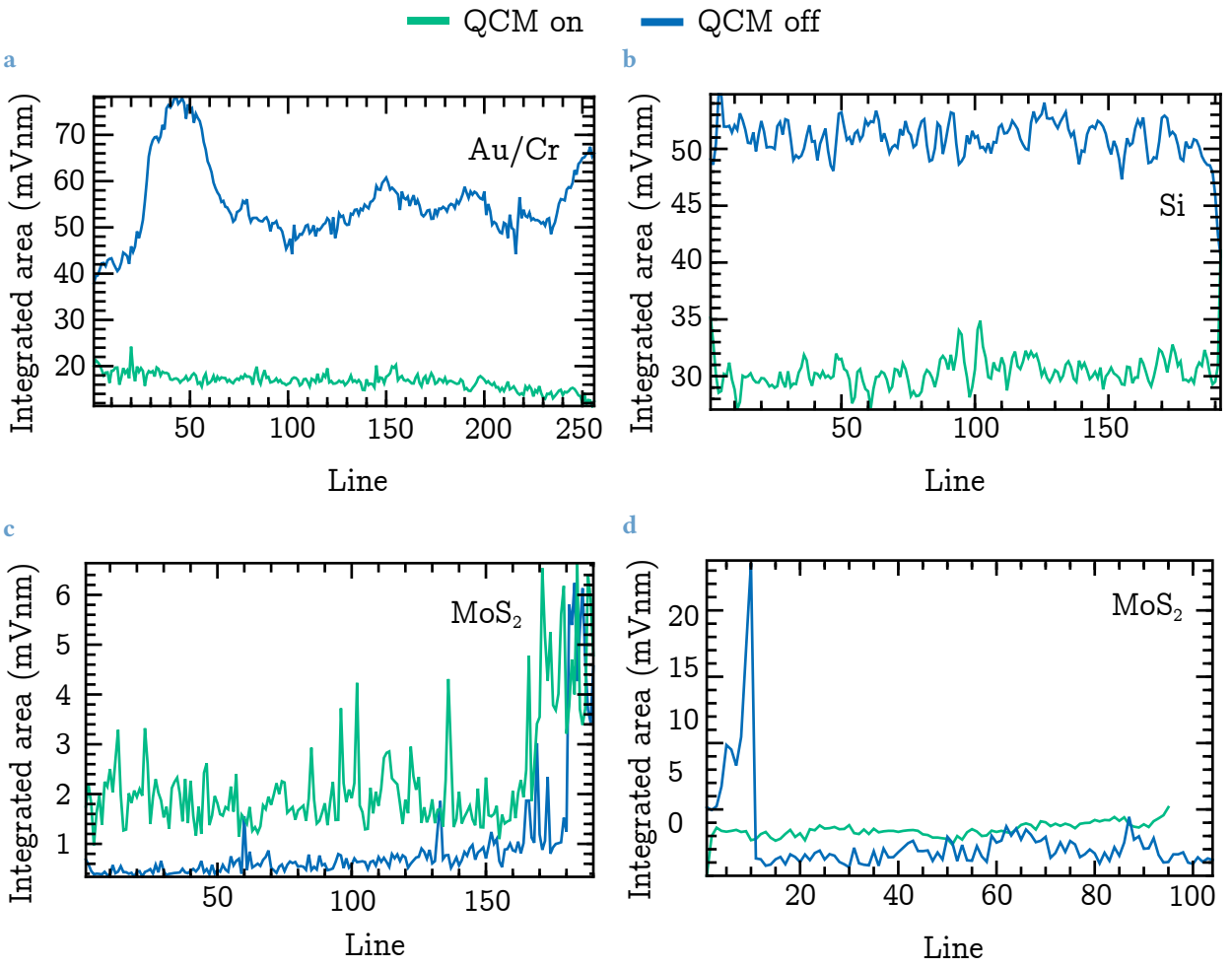

Figure 3. Wear friction profile - Integrated lateral signal as a function of the measurement line for **(a/d)** Au/Cr, Si and MoS_2. The area of the force loop is directly proportional to the friction force during sliding. The green and blue line indicate if the the state of the QCM. The large deviation from the mean friction in **(a) (b)** and **(c)** stems from a surface irregularity, a step edge and the powering off of the QCM, respectively

experiments with the same sample have shown results varying from no apparent alteration of the friction profile to complete elimination of friction.

It is hypothesised that these results arises from differences in the angle of the crystal oscillatory direction relative to the fast scanning direction of the cantilever, as shown in Figure 5b. The shear mode vibration creates a friction force, F_{QCM}, between the tip apex and the substrate parallel to direction of oscillation. For all angles θ between 0 and π this friction force has a non-zero vector parallel to the fast scanning direction of the cantilever. This would in part explain the different friction responses of the same sample, since only the parallel components can be measured by the cantilever. Thus, the angle dependent term $F_{QCM}sin\theta$ is introduced. Note that the proposed theory would however suggest that the QCM always increases friction for any angle

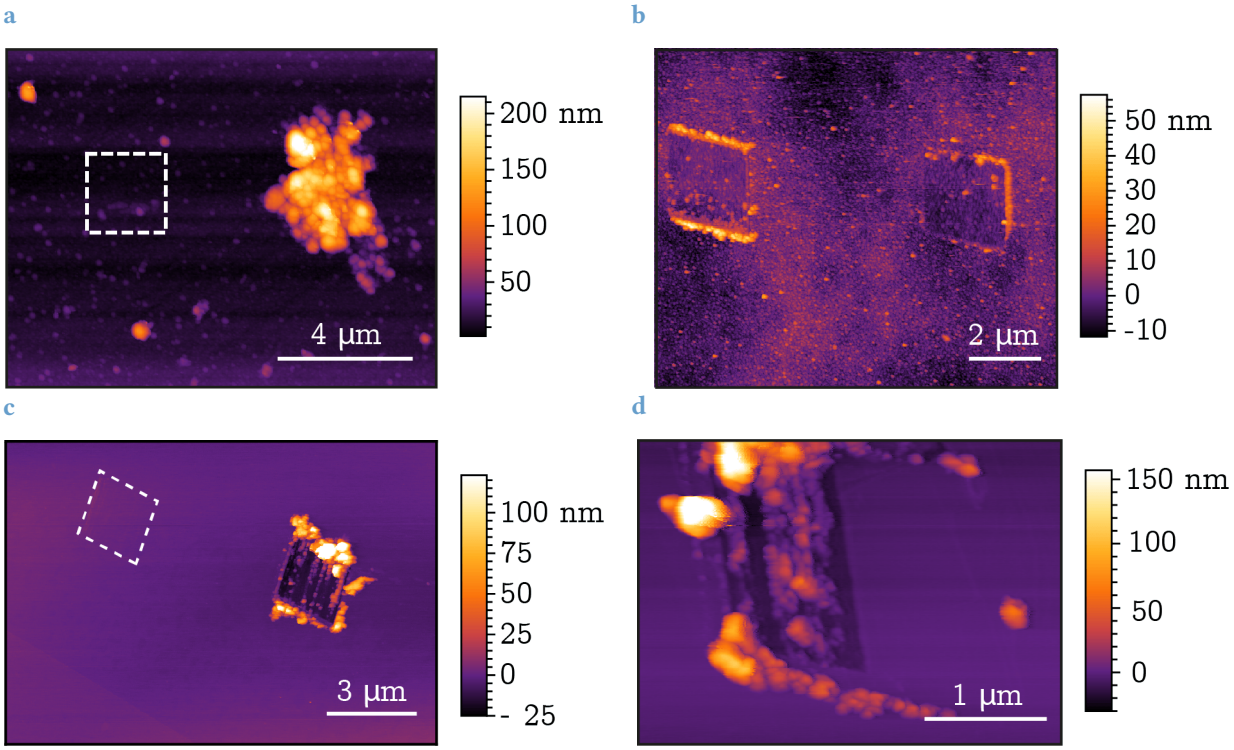

Figure 4. Substrate wear - AFM topographic images of the substrate after wear with and without QCM vibrations. **(a)** On the left hand side is the affected area of the *Au substrate with the QCM off*, as indicated by the white dashed square. There is no apparent surface damage visible. On the right hand side *Au substrate with QCM enabled.* The surface shows substantial wearing when coupled to an active QCM. **(b)** Si substrate with on the left the *QCM worn surface* and on the right *without the QCM* . Similarly, the **(c,d)**. Show the MoS_2 sample. In the *absence of the QCM* the surface was unaltered with respect to the surroundings, indicated by the area enclosed in the white dashed square. *MoS_2 substrate with QCM on* **(d)** Shows a single run where *halfway the QCM is turned off.* The debris on the right hand side originates from the damaged surface

other than 0 or π. Therefore it is expected that the vibration bring about another means of friction reduction, such that the sum of the parallel QCM friction vector and this processes have interval of θ for which they are positive and for which they are negative. This is plotted schematically in Figure 5b. Possible mechanism will be further elaborated on in the next section.

3.2 Substrate Wear

The topography of the samples is shown in Figure 4. Note that the adhered substrate samples (Si and MoS_2) were unstable over the time span of high resolution imaging. Consequently, the samples drifted causing image artifacts, under which a compression of the image along the slow scanning direction and distortion of the internal angles. To account for this bias, image analysis was preceded by re-scaling of the images to better represent the true geometry. From the images

it is apparent that surface damage becomes more severe when wearing is performed with the QCM turned on, shown in Figure 4b and 4d on the left hand side and in Figure 4a and 4c on the right hand side. Especially, for Au/Cr and MoS_2 this hold, with no visible damage on the Au/Cr substrate and little for MoS_2, as can be seen for the area enclosed in the white dashed square in Figure 4a and 4c. The Integrated volume for Au/Cr amounts to 28 and 1417 nm^3 when the QCM is turned off and on, respectively. The wear in absence of the QCM is believed to be below the detection limit and hence the volume is largely attributed to the irregular surface. For MoS_2 these volumes amount to 6.8 and 276 nm^3. The increase in wear is remarkelbly lower for the Si substrate with respect to the others. The wear increases from 15 to 70 nm^3, a factor of 4.7. The differences in wear increase among the different samples are in part due to the packing of the debris and the position of the sample on the crystal.

The stark increase in surface damage is attributed to the increased sliding distance the tip makes under the 5MHz oscillation. The path length can be considered to consist of two components; the extra path length arising from the crystal oscillations and the distance travelled by the probe during regular scanning. The latter is given by:

$$x_{scan} = 2N_{lines}w_{scan} + h_{scan} \tag{3.1}$$

Where N_{lines} are the number of scan lines, the factor 2 accounts for every scan line being covered during trace and retrace, w_{scan} is the width of the scan, coinciding with the fast travel direction and h_{scan} is the height of the scan, corresponding to the slow scan direction. Similarly, the path covered by the QCM vibrations can be calculated according to the relation:

$$x_{QCM} = \left(\frac{N_{lines}\omega}{2\pi f_{scan}}\right) 2u(r_{sample}, \frac{1}{4\omega}) \tag{3.2}$$

Where f_{scan} is the scan rate of the tip in the fast scanning direction and r_{sample} is the radial sample location. The first terms encompasses the number of oscillation cycles the QCM crystal makes during a single sliding experiment. For the displacement profile we take $\frac{1}{4\omega}$ as time input to –a fourth of the oscillation time– as this is one half of displacement experienced by the sample at r_{sample} within one oscillation cycle. The factor 2 is simply to account for the fact twice the amplitude is covered during a cycle.[3] The path length components for every sample are displayed in Figure 5b. It becomes clear that the path length in dominated by the QCM oscillations, which is 4 orders of magnitude greater than the scanning distance. Hence, even though the friction is reduced by a factor of 2 to 3, there is still a net increase in wear.

As previously hypothesised the vibrations potentially trigger a friction reduction pathway. A possible candidate could be the large number of worn particles generated by the QCM vibrations. The introduction of third bodies between two interfaces has been shown to be beneficial in reducing friction.[15,16] Based on Figure 4d it is reasonable to assume that the debris interacts with the tip. The wearing of MoS_2 is negligible when the QCM is turned of but still we see large fragments at the border of the "QCM off" area.

[3] This introduces a minor error, while we consider the oscillation not by time but by cycle. this is justified however, by the negligible small fraction the uncompleted cycle posses with respect to the total number of completed cycles

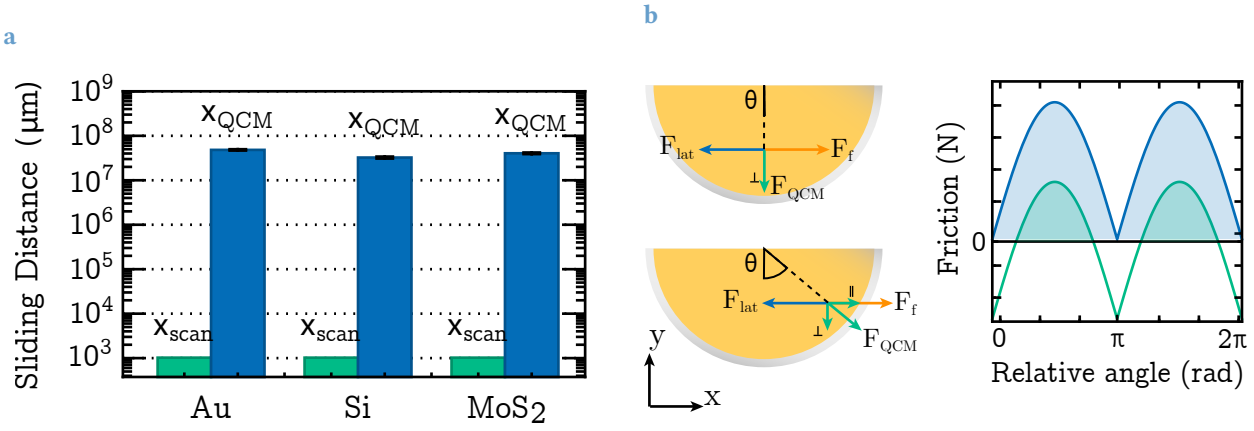

Figure 5. Vector splitting & path length - (a) The sliding distance per sample. x_scan shows the path-length of the patterning motion in teh absance of QCM vibrations. x_{QCM} shows the contribution to the path length due to the crysal displacement. **(b)** Schematic representation of the forces the tip experiences during sliding. When θ is 0 the additional friction from cause by the QCM vibration (green vector) is orthogonal to the the measurement direction of the cantilever (blue vector). For any angle between 0 and π there is a positive contribution to the sliding friction (orange vector) by the parallel (∥) QCM vector. The plot shows the additional friction induced by the QCM. The blue curve represents the QCM friction as a function of the angle between oscillation and cantilever motion. The green curve represents the same friction force plus a constant friction reduction induced by the QCM.

It is however difficult to make any definitive statements about the mechanism. Firstly, The large friction increase for MoS_2 challenges the proposed view as it is commonly used as a dry lubricant. Though if the particles are sufficiently small, a large edge to surface ratio might cause a high degree of oxygen attachment on edge sites. This would result in increased coefficients of friction.[17] Moreover, since we have only observed an angle dependent friction responses in preliminary experiments for MoS_2 and a small and not properly defined subset of angels, we should note that careful assessment of the other samples is in order. Especially, because friction anisotropy of crystal surfaces to some extend underlies our observations.[18]

4 Conclusion

In this report we have demonstrated that the use of a QCM to induce vibrations, results in substantially increased surface wear, even if the friction during sliding contact is lowered by the QCM. This means that our findings go against the general assumption that QCM-induced friction reduction coincides with a lowering interface degradation.[9] This wear increase is attributed to the additional sliding distance originating from the rapid crystal displacement of the QCM crystal. The latter being in the order of 10^7 μm compared to the 10^3 μm caused by regular sliding. Other works seem to disregard this vast rise in sliding distance, as no mention of it is found in the context of friction or wear.

Further, we observed several friction responses with regard to vibrations, ranging from a reduction to an increase. Especially, the increase in friction is peculiar, because our preliminary experiments on MoS_2 have only shown the friction to decrease or completely disappear. Furthermore, there is no mention in any literature of a raise in friction caused by QCM vibrations, only in total or partial decreases.[6,9,11] These result have lead us to hypothesise that the measured friction is connected to the relative position of the sample on the electrode as well as a a friction decrease triggered by the QCM oscillations. However, our study does not pose any closing evidence for this hypothesis and thus is further research required. Several experiments to test our theory are outlined in the subsequent section.

With regards to the experimental setup, although AFM has not been frequently used for similar experiments by others, it proves to perform well for analysis of the wear friction relationship. This is mainly due to the ability to alter the sample in contact mode and subsequently analyse surface topography in tapping mode with high spatial resolution. It is thus advised to continue with the current setup.

5 Outlook

Based on the results and discussion presented in this report, several follow up experiments are proposed to gain a better insight in the raised hypothesis:

- As hypothesised, the debris could possibly act as a lubricating layer between tip and substrate. To test the influence of the debris as solid lubricant, one could perform a similar experiment as in this study, but interchanging the square wear pattern for a $30\mu m$ non-reciprocal stroke, as shown in Figure 6a. The plowing of the tip over the surfaces will cause debris formation to be expelled to the side and behind the tip. Hence, this setup prevents the tip from sliding over loose debris from the previous strokes, allowing for analysis of the friction in absence of newly created third bodies. Care has to be taken that no debris is adhered to the tip when performing a new non-reciprocal line experiment. To this end it is advised to clean the tip between every single line.[19]

- The undefined relative orientation between tip sliding and QCM oscillation introduces large uncertainty. This makes it difficult to determine the origin of the observed friction behaviour. In order to better understand the angle dependence of the surface wear and friction profile, the experiments must be repeated under various angles. Figure 6b shows a schematic model of the custom designed rotating QCM holder. The body of the apparatus can remain stationary while the crystal and rotating plate can be rotated freely over 360°. The markings on the holder allow for 3° angular resolution. Follow the experiments should be carried out over an angle of 180° with at most 10° increments. For higher increments not enough data per angle is collected to draw meaningful results. As pointed out in Section 3 the friction anisotropy of crystal surfaces has to be taken into account the process. Therefore, it is advised to study the phenomenon first on amorphous samples to isolate the extend of the QCM friction anistropy.

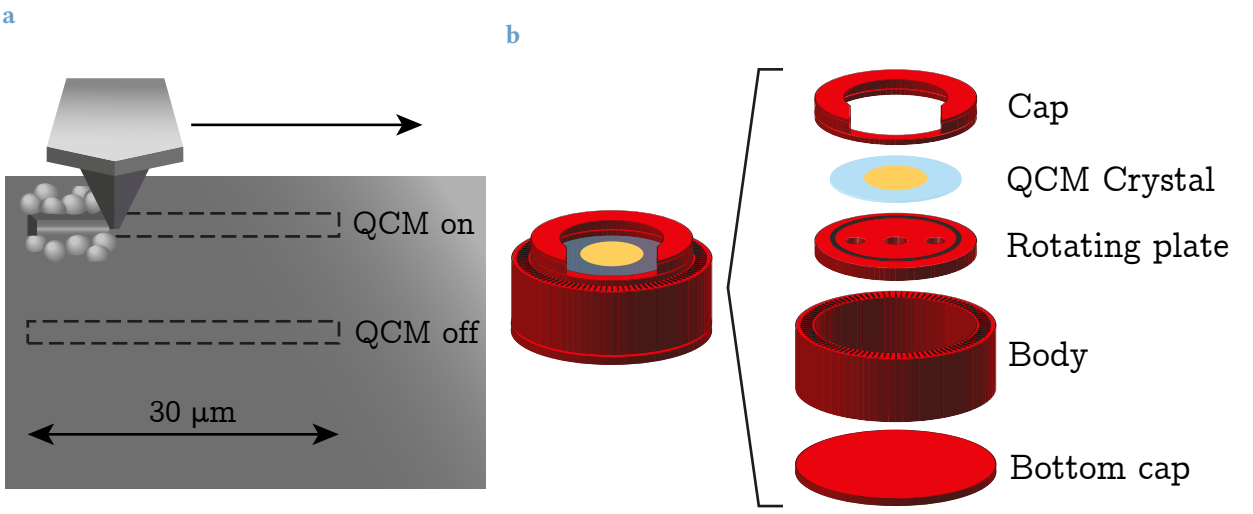

Figure 6. Continuation experimental work - **(a)** Schematic outline of the non-reciprocal sliding experiment. The tip slides over the sample in a single 30 μm line with constant velocity, varying the use of the QCM per line. The loose debris particles from the surface are created behind the tip and thus it will not be picked up, excluding lubrication by the debris. **(b)** Model of the the rotating QCM holder. The rotating plate is designed such that the body remains stationary, while the rotating plate –with the attached crystal– can rotate freely. The angle increments are spaced 3° apart

- In the current study only the substrate is analysed. However, it is interesting to also monitor tip topography over the course of the experiments, as to see if the wear increase only takes place on the substrate or also on the sample. To this end analysis of the probe with scanning electron microscopy might prove useful to map the evolution of the tip between every other wear site. It is insightful to extend this analysis with energy dispersive x-ray spectroscopy of the substrate and tip, to get a quantitative and qualitative understanding of the source of the debris. Especially, experiments with the diamond coated tip lend themselves well for such analysis, while a clear distinction in the elemental fingerprints of substrate and tip can be observed.

References

[1] Berman, D.; Erdemir, A.; Sumant, A. V. *ACS Nano* **2018**, *12*, 30.

[2] Jost, P. *Proc mechanical failures prevention group* **1976**, 117–139.

[3] Gnecco, E.; Bennewitz, R.; Pfeiffer, O.; Socoliuc, A.; Meyer, E. In *Nanotribology and Nanomechanics*; Springer, 2008; pp 557–605.

[4] Stoyanov, P.; Chromik, R. R. *Materials* **2017**, *10*, 550.

[5] Borovsky, B. P.; Garabedian, N. T.; Mcandrews, G. R.; Wieser, R. J.; Burris, D. L. **2019**.

[6] Seed, C. M.; Acharya, B.; Andrus, R.; Krim, J. *Sensors and Actuators, A: Physical* **2020**, *306*, 111913.

[7] Borovsky, B.; Mason, B. L.; Krim, J. *Journal of Applied Physics* **2000**, *88*, 4017–4021.

[8] Ishikawa, M.; Wada, N.; Miyakawa, T.; Matsukawa, H.; Suzuki, M.; Sasaki, N.; Miura, K. *RAPID COMMUNICATIONS PHYSICAL REVIEW B* **2016**, *93*, 201401.

[9] Bhattacharjee, A.; Garabedian, N.; Borovsky, B.; Burris, D. L. **2021**.

[10] Dayo, A.; Alnasrallah, W.; Krim, J. *Physical Review Letters* **1998**, *80*, 1690.

[11] Wada, N.; Ishikawa, M.; Shiga, T.; Shiomi, J.; Suzuki, M.; Miura, K. *Physical Review B* **2018**, *97*, 161403.

[12] Green, C. P.; Lioe, H.; Cleveland, J. P.; Proksch, R.; Mulvaney, P.; Sader, J. E. *Review of Scientific Instruments* **2004**, *75*, 1988–1996.

[13] Martin, B. A.; Hager, H. E. *Journal of Applied Physics* **1989**, *65*, 2630–2635.

[14] Johannsmann, D.; Heim, L. O. *Journal of Applied Physics* **2006**, *100*, 1–6.

[15] Singer, I.; Dvorak, S.; Wahl, K.; Scharf, T. *Journal of Vacuum Science & Technology A: Vacuum, Surfaces, and Films* **2003**, *21*, S232–S240.

[16] Lancaster, J. *Tribology International* **1990**, *23*, 371–389.

[17] Savan, A.; Pflüger, E.; Voumard, P.; Schröer, A.; Simmonds, M. *Lubrication Science* **2000**, *12*, 185–203.

[18] Vazirisereshk, M. R.; Hasz, K.; Carpick, R. W.; Martini, A. *Journal of Physical Chemistry Letters* **2020**, *11*, 6900–6906.

[19] Sirghi, L. *Rom. J. Phys* **2011**, *56*, 144.

[20] Voigtländer, B.; *NanoScience and Technology Scanning Probe Microscopy Atomic Force Microscopy and Scanning Tunneling Microscopy*; Tech. Rep..

[21] Giessibl, F. J.; Hembacher, S.; Bielefeldt, H.; Mannhart, J. *Science* **2000**, *289*, 422–425.

[22] *AFM: Background information — MyScope*. https://myscope.training/legacy/spm/background/.

[23] *AFM Lesson 14 - Friction loops and Lateral Force Microscopy (LFM) - YouTube*. https://www.youtube.com/watch?v=n-ZFfQwecSg.

Appendices

A Atomic Force Microscopy

Atomic force microscopy is an analysis tool, which captures the properties of surfaces. The technique is a subset of the scanning probe microscopy (SPM), which use the use the interaction between a probe an the substrate to map the local material properties. Commonly, the data is represented in an image by, which can be constructed via raster scanning of the substrate. Using this technique it is possible to achieve sub-atomic scale resolution.[20, 21]

The working principal of AFM is based around measuring the force between the sample and the tip, visualised in Figure A.1. From the qualitative plot three force regimes can be distinguished. Firstly, when the tip sample distance is large, their is no appreciable force acting between the tip and substrate. For smaller separations a negative i.e. attractive force is pr sent between the tip and sample. Lastly, if the tip approaches the sample to closely a strong positive i.e. repulsive force occurs between tip and sample.

To quantify the force the cantilever is treated as a simple spring. The force acting on the cantilever can then be correlated to the deflection of the cantilever via Hook's law:

$$F = k_{cant} z \tag{A.1}$$

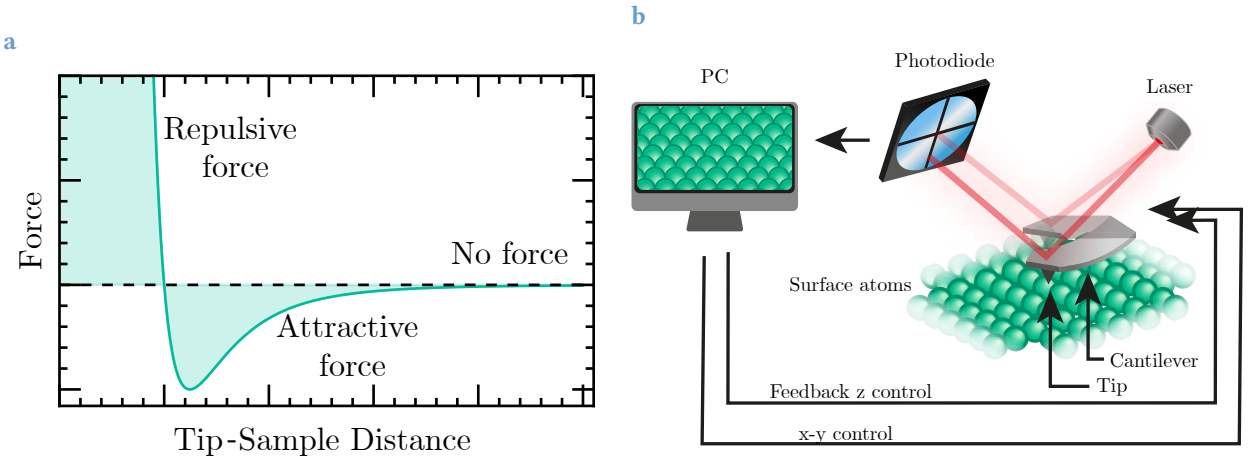

Figure A.1. AFM working principle - (a) Qualitative plot of the forces acting between an AFM probe and the substrate surface. When the separation becomes smaller the interaction results in an attractive force, signified by the graph being substantially below the x-axis. When separation is reduced further repulsive forces from overlapping electrons clouds start to contribute resulting in repulsion between the tip and sample.The force distance curve is modeled after the derivative of the Lennard-Jones potential. Figure adapted from "Scanning Probe Microscopy" .[20] **(b)** Schematic representation of an atomic force microscope. The lateral movement and vertical displacement is driven by the PC. To maintain the set top-sample force a feedback loop control the z position of the cantilever. The deflection i.e. tip sample forces, of the cantilever are measured via a position sensitive photo diode. Figure adapted from "MyScope".[22]

Where z is the displacement of the cantilever with respect to its equilibrium position and k_{cant} is the spring constant of the cantilever. The deflection is normally monitored with a laser and a split photodiode. In the absence of any applied forces the angle between the laser beam and the sensor is θ_1. During measurement the tip sample forces vary resulting in changes in deflection. Subsequently, the angle the laser light makes with respect to the back of the cantilever and photodiode changes to θ_2. The difference between the angles allows to monitor the forces acting on the tip, as visualized in Figure A.1b

Mapping of the surface features can be performed by operating the the AFM in the attractive or repulsive force regime. When the AFM is operated using the latter, one speaks of contact mode. The feedback loop procedure in this mode, relies on maintaining a set force and correspondingly a constant tip-sample distance. If the probe-substrate interactions are sufficiently strong, because of high force set points and/or weak intra-substrate bonds, the measurements might induce plastic deformation of the sample.

Alternatively, the AFM can also operate dynamically in the attractive regime. In this so called tapping mode, the cantilever is excited to oscillate near it natural frequency. When the tip approaches the substrate, a change in the resonance frequency is brought about the interactions with the surface. Correspondingly, the amplitude of oscillation is changed. The feedback loop operates by trying to keep the amplitude and hence the force constant.

A.1 Lateral Force Microscopy

Contact mode experiments can be extended to not only provide z-data but also about in plane forces, this technique is known as lateral force microscopy (LFM). If the tip is in contact with the sample, friction between the tip and substrate interface will induce lateral forces on the tip apex. When the fast scanning direction is orthogonal to the cantilever length, this will result in torsional bending of the cantilever. These forces can be recorded by special quadratic photodiodes, as shown in Figure A.1b. These measurements are able to provide insight about the local friction during sliding under various experimental condition e.g. applied force and sliding speed. Often, the energy lost through dissipation results in physically alteration of the surface. This manifest itself as plastic deformation, as well as the initiation and propagation of cracks or material fatigue. Consequently, loose wear debris is formed. Such debris formation originating from friction induced wearing can often be tracked through changes in the friction response of the surface. Moreover, correlations between wear and friction can be studied by subsequent scanning of the section in tapping mode. Accordingly, LFM is a powerful tool for studying friction and wear behaviour of materials.

A.2 Relation Lateral Force and Integrated Force Loop

Consider a tip sliding over a surface with an incline of θ at constant velocity a horizontal cantilever and no adhesion, as visualised in Figure A.2a. In the absence of acceleration the net

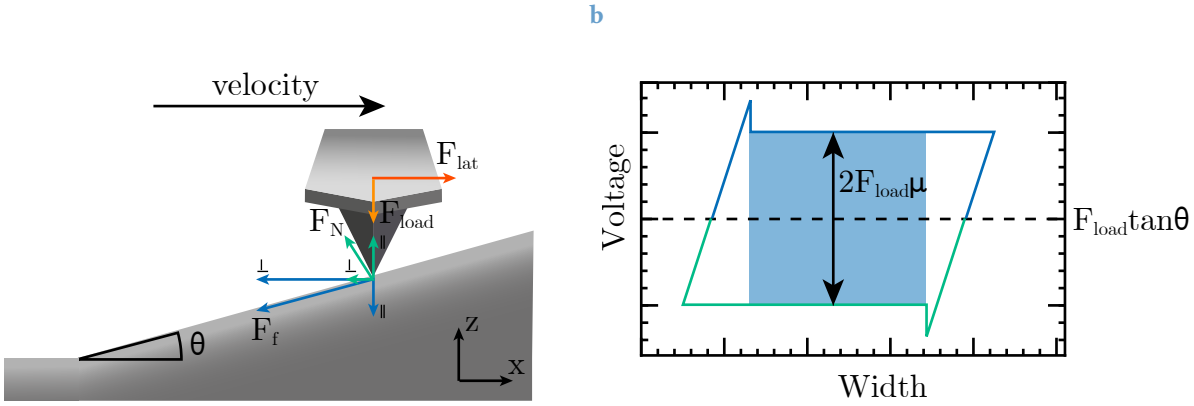

Figure A.2. Tip forces - **(a)** AFM probe in contact sliding at a constant speed over a slanting surface with a slope of θ °. The blue, green orange and dark orange vectors represent the friction force (F_f),normal force (F_N), lateral force (F_{lat}) and loading force (F_{load}), respectively. The friction and normal force are made up of basis vectors parallel ($\parallel$) and perpindicualar ($\perp$) to the x-axis. Figure recreated from "Friction loops and Lateral Force Microscopy (LFM)".[23] **(b)** Schematic representation of a friction force loop as would be measured on a surface with constant slope and coefficient of friction. The blue and green line represent the trace and retrace, respectively. The blue shaded area is the the integral of the force loop excluding the dynamical friction regime. The numerical value of the mean of the force loop is proportional to the applied load and angle of the slope. The Euclidean distance between the mean and the trace/retrace is proportional to the applied load and the coefficient of friction.

force on the system is given by:

$$\sum_i F_i = 0 \tag{A.2}$$

Similarly all orthogonal components of the net force i.e. the x and z direction, should be equal to 0 resulting in:

$$\sum F_x = F_{lat} - F_N sin\theta - F_f cos\theta = 0 \tag{A.3}$$

$$\sum F_z = F_{load} - F_N cos\theta - F_f sin\theta = 0 \tag{A.4}$$

Where F_{lat} describes the force displacing the tip over the surface, F_{load} is the force corresponding to the applied load, F_N is the normal force and F_f is the friction force, respectively. Substitution of Equation A.3 in Equation A.4 and using the assumption that friction forces scale linearly with the normal force – $F_f = \mu F_N$ – leads to:

$$F_{lat}^{+} = F_{load}\left(\frac{tan\theta + \mu}{1 - \mu tan\theta}\right) \tag{A.5}$$

$$F_{lat}^{-} = F_{load}\left(\frac{tan\theta + \mu}{1 + \mu tan\theta}\right) \tag{A.6}$$

Here the plus and minus sign indicate the tip climbing or descending the slope. The proportionally constant μ is the coefficient of friction. In the limit of a low value for the slope and friction coefficient i.e. $tan\theta < 1$ and $\mu < 1$, $\mu tan\theta << 1$, hence reducing Equations A.6 and A.5 to [4]:

$$F_{lat}^{\pm} = F_{load}(tan\theta + \mu) \tag{A.7}$$

The above Equation captures the features of the static friction regime of the force loop. The mean of the loop is given by the term $F_{load}tan\theta$, whereas the distance between the trace/retrace and the mean is equal to $F_{load}\mu$, which is shown in Figure A.2b. With Figure A.2a and Equation A.7 one can easily deduct that for small values of θ the lateral force is roughly opposite and equal of the friction force, so that the the friction force is proportional to the applied load and the coefficient of friction. This capture in the relation:

$$F_f \approx F_{load}\mu \tag{A.8}$$

Similarly the integrated area of the static force regime is proportional to the friction force.

[4] This is a reasonable assumption considering that the surface roughness of the substrates in our experiments was small and that common values for μ are in the order of

B Material Overview

Table B.1. Substrate and Instruments used and their respective retail details

Materials	**Retailer**	**article code**
Single crystal MoS_2	Merck, Research Development Production	808652
5 MHz QCM crystal sensor	INFICON	149273-1
AFM probe	Bruker	CONTVA-A
AFM	Bruker	Dimension Icon
AFM probe	Bruker	RTESPA-300
diamond-coated AFM probe	Adma Inovations	NC-LC
Maxtek RQCM system	INFICON	N.A.
CHK-100 QCM holder	INFICON	184204